Iranian Journal of Organic Chemistry Vol. 7, No. 1 (2015) 1463-1472

Molecular modeling of most stable configurations of azocubane: DFT study of structural and energetically properties

Mehdi Nabati* and Mehrdad Mahkam

Chemistry Department, Faculty of Science, Azarbaijan Shahid Madani University, Tabriz, Iran.

Received: December 2014; Revised January 2015; Accepted: January 2015

Abstract: Density functional theory (DFT) calculations have been used to investigate the structural properties, dipole moments, polarizabilities, Gibbs energies, hardness, electronegativity, HOMO/LUMO energies, chemical potentials, density of states and detonation properties of trans and cis configurations of azocubane. All properties have been obtained using the B3LYP functional and 6-31G(d,p) basis set. Also, IR, UV-Vis, CD and NMR spectra of the structures were simulated. The volumes of the structures computed to get the densities of the molecules. All calculations carried out in gas phase at temperature 293.15 k and pressure 1 atm. The simulation results revealed that the trans configuration of azocubane exhibits more stability, low reactivity and more detonation property as compared to the cis trans configuration of azocubane.

Keywords: Azocubane, Cis and trans configurations, DFT study, Stability, Reactivity.

Introduction

Cubane, first appeared on the scientific research stage after painstaking experimentation and was conclusively synthesized by Eaton and Cole in 1964 [1]. As befits the symmetry and accompanying esthetics, large strain energy and eight tertiary carbons all capable of possible functionalization, the chemistry of this seemingly simple eight-carbon hydrocarbon (C_8H_8) and its derivatives has blossomed. Cubane's heat of formation (+149 kcal/mol), density (1.29 g/cm^3), and strain energy (+166 kcal/mol) are extraordinarily high, a combination not exceeded by any other stable hydrocarbon available in reasonable quantities [2]. The addition of groups that are energy-rich, oxidizing, or both will create exceptionally dense and powerful explosives, propellants, and fuels [3]. The applications of cubane can be divided into the following categories: the explosives industry, pharmaceuticals, polymer science [4]. Cubane's potential as a source of high-energy explosives was first recognized in the early 1980s when Gilbert of the U.S. Army Armament and Development Command (now ARDEC) pointed out that the properties of cubane could make certain cubane derivatives important explosives [5]. Explosives and medicines are as different as night and day. One destroys life while the other attempts to save life. For example, a dipivaloylcubane –a cubane derivatized with keto, cyano, and amide groups- exhibits moderate activity against human immunodeficiency virus (HIV), which causes AIDS, without impairing healthy cells [6]. In addition, a phenylcubane has shown moderate anti-cancer activity [7]. Cubane polymers, due to their well-defined dimensionality and rigid geometry, could prove to be important building structures in the developing world of nanoarchitecture, in the form of oligomeric compounds [8].

Azo compounds are compounds bearing the functional group R-N=N-R', in which R and R' can be either aryl or alkyl. The more stable derivatives contain

*Corresponding author. Tel: (+98) 413 4327501, Fax: (+98) 413 4327501, E-mail: mnabati@ymail.com

two aryl groups [9]. The N=N group is called an azo group. The name azo comes from azote, the French name for nitrogen that is derived from the Greek a (not) + zoe (to live) [10]. As a consequence of π-delocalization, aryl azo compounds have vivid colors, especially reds, oranges, and yellows. Therefore, they are used as dyes, and are commonly known as azo dyes [11]. Aliphatic azo compounds (R and/or R' = aliphatic) are less commonly encountered than the aryl azo compounds [12]. A commercially important alkyl azo compound isazobisisobutyronitrile (AIBN), which is widely used as an initiator in free radical polymerizations and other radical-induced reactions. It achieves this initiation by decomposition, eliminating a molecule of nitrogen gas to form two 2-cyanoprop-2-yl radicals [13].

One of the most intriguing properties of azo compounds is the photoisomerization of trans and cis isomers [14]. The two isomers can be switched with particular wavelengths of light: ultraviolet light, which corresponds to the energy gap of the π-π* (S_2 state) transition, for trans-to-cis conversion, and blue light, which is equivalent to that of the n-π* (S_1 state) transition, for cis-to-trans isomerization [15]. For a variety of reasons, the cis isomer is less stable than the trans (for instance, it has a distorted configuration and is less delocalized than the trans configuration) [16]. Thus, cis-azo compound will thermally relax back to the trans via cis-to-trans isomerization [17].

Nowadays, azocubane wasn't synthesized. In the present work, we report the theoretical study of the stability, reactivity, electron transitions and photoisomerization and detonation properties of azocubane isomers. There is no doubt that the density functional theory (DFT) methods are now established computational techniques for the evaluation of structural and energetic properties of various chemical systems [18]. Here, we used B3LYP/6-31G(d,p) method for all calculations.

Results and discussion

Scheme **1** shows the structure of cis and trans isomers of azocubane (CAC and TAC, respectively) and their atomic numbering.

The geometry optimized structures of the molecules computed at the B3LYP/6-31G(d,p) level of theory are presented in Figure **1**.

Geometrical parameters containing bond lengths, bond angles, and dihedral angles are listed in Table **1**. From the data, the N-N bond distance (1.257 Aº) in trans isomer (TAC) is longer than the N-N bond distance (1.250 Aº) in cis isomer (CAC). In contrast, the N1-C2 bond length of CAC (1.440 Aº) is longer than the N1-C2 bond length of TAC (1.424 Aº). The results of the calculations indicated that, in CAC system the longest bond among all the bonds corresponds to the C2-C5 bond of molecule, which is 1.589 Aº, and the shortest one is 1.088 Aº for C5-H bond of the molecule. In contrast, the longest bonds of trans isomer (TAC) are C2-C6 and C2-C3, which are 1.579 Aº, and the shortest bond is 1.088 Aº for C5-H bond of the structure. And also, we can see the N-N-C bond distance of CAC is longer than the N-N-C bond length of TAC, which are 125.427 degree and 113.686 degree respectively. It was obtained that the C-N-N-C torsion angle for cis configuration is longer than the one of trans configuration.

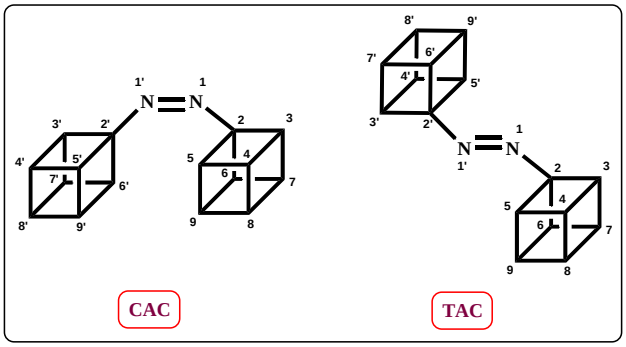

Scheme 1: Structures of azocubane isomers.

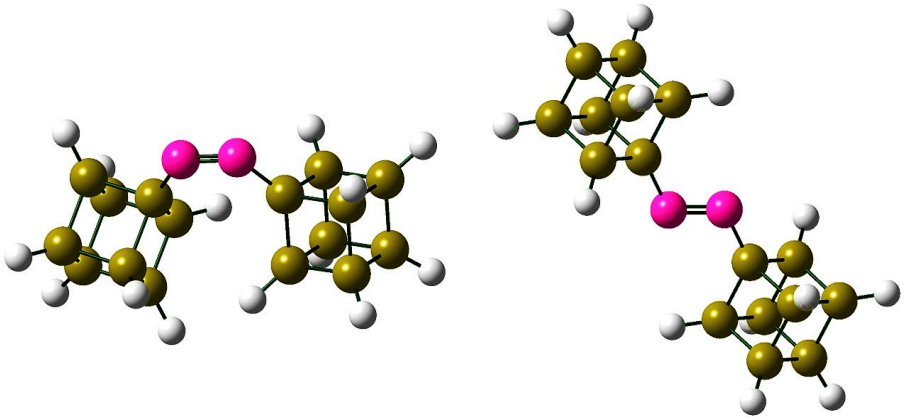

Figure 1: The geometry optimized (B3LYP/6-31G(d,p)) structures of present concern.

Table 1: Bond lengths (Aº), bond angles (degree) and dihedral angles (degree) at B3LYP/6-31G(d,p) for azocubane isomers.

Bonds (Aº)	CAC	TAC	Angles (degree)	CAC	TAC
N-N	1.250	1.257	N-N-C	125.427	113.686
N1-C2	1.440	1.424	N1-C2-C3	117.621	122.357
C2-C3	1.569	1.579	N1-C2-C5	134.812	122.336
C3-C4	1.566	1.570	N1-C2-C6	123.412	130.391
C4-C5	1.568	1.571	C2-C3-C4	90.144	90.333
C2-C5	1.589	1.567	C3-C4-C5	90.707	90.073
C2-C6	1.587	1.579	C4-C5-C2	89.325	90.334
C3-C7	1.567	1.567	C3-C2-C5	89.820	89.252
C4-C8	1.570	1.571	C3-C2-C6	89.128	90.617
C5-C9	1.569	1.571	C5-C2-C6	89.606	90.615
C6-C7	1.568	1.567	C2-C3-C7	90.814	89.100
C7-C8	1.570	1.570	C4-C3-C7	90.302	90.227
C8-C9	1.569	1.571	C3-C4-C8	89.853	89.889
C6-C9	1.569	1.570	C5-C4-C8	90.283	89.887
C3-H	1.090	1.090	C4-C5-C9	89.734	90.232
C4-H	1.091	1.091	C2-C5-C9	89.658	89.103
C5-H	1.088	1.088	C7-C6-C9	90.110	89.782
C6-H	1.090	1.090	C-N-N-C	-1.424	179.995
C7-H	1.090	1.090	N-N-C2-C3	-159.304	123.817

C8-H	1.090	1.091	N-N-C2-C5	-38.318	-123.677
C9-H	1.091	1.091	N-N-C2-C6	91.755	0.053

Natural bond orbital (NBO) analysis data of the structures are listed in Table **2**. Natural bond orbitals (NBOs) are localized few-center orbitals that describe the Lewis-like molecular bonding pattern of electron pairs in optimally compact form. More precisely, NBOs are an orthonormal set of localized "maximum occupancy" orbitals whose leading *N*/2 members (or *N* members in the open-shell case) give the most accurate possible Lewis-like description of the total *N*-electron density. This analysis is carried out by examining all possible interactions between "filled" (donor) Lewis-type NBOs and "empty" (acceptor) non-Lewis NBOs, and estimating their energetic importance by second-order perturbation theory [19]. As can be seen from the data of Table **2**, more p orbitals are used to formation of sigma N-N bond in TAC structure to CAC compound. To formation of pi N-N bond, both structures have used from pure p orbitals. In CAC and TAC, the nitrogen and carbon atoms are participated with sp^2 and $sp^{2.5}$ hybrids, respectively in formation of N-C bond. The hybrids of participating atoms of C-C bonds show that the cubane section is under strain. For this reason, Carbon atoms use more p orbitals ($sp^{3.3}$-$sp^{3.6}$). And also, cabon atoms use low p orbitals to formation of C-H bonds in cubane section of compounds. It can be deduced the hydrogen atoms are acidic property.

Table 2: Natural bond orbitals (NBOs) population analysis at B3LYP/6-31G(d,p) for azocubane isomers.

Bonds	Compound	Occupancy	Population/Bond orbital/Hybrids
σ(N1-N1`)	TAC	1.98470	50.00% N1 ($sp^{2.35}$), 50.00% N1` ($sp^{2.35}$)
	CAC	1.99153	50.00% N1 ($sp^{2.05}$), 50.00% N1` ($sp^{2.05}$)
π(N1-N1`)	TAC	1.94523	50.00% N1 (p), 50.00% N1` (p)
	CAC	1.95471	50.00% N1 (p), 50.00% N1` (p)
σ(N1-C2)	TAC	1.98471	58.79% N1 ($sp^{2.03}$), 41.21% C2 ($sp^{2.51}$)
	CAC	1.99158	57.75% N1 (sp^{2}), 42.25% C2 ($sp^{2.52}$)
σ(C2-C3)	TAC	1.94858	50.95% C2 ($sp^{3.40}$), 49.05% C3 ($sp^{3.50}$)
	CAC	1.94474	51.30% C2 ($sp^{3.39}$), 48.70% C3 ($sp^{3.59}$)
σ(C3-H)	TAC	1.99287	63.20% C3 ($sp^{2.18}$), 36.80% H (s)
	CAC	1.99275	63.33% C3 ($sp^{2.18}$), 36.67% H (s)

The molecular electrostatic potential (MEP) is the force acting on a positive test charge (a proton) located at a point in the vicinity of a molecule through the electrical charge cloud generated through the molecules electrons and nuclei [20]. The three-dimensional electrostatic potential maps of the structures are shown in Figure **2**. The red loops and the green loops indicate negative and positive charge development for a particular system respectively. As can be seen from the figures the negative charge is located on the nitrogen elements as expected due to the electron withdrawing character of theirs and positive charge is located on the cubane sections of the structures.

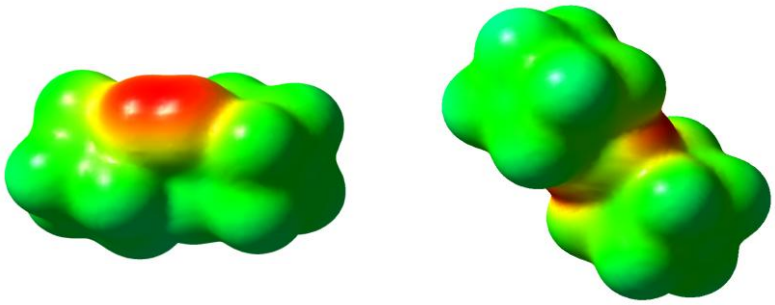

Figure 2: The 3-D electrostatic potential maps of CAC (left image) and TAC (right image).

The NMR analysis is an important property of a compound, and also an effective measure to identify structures [21]. Here, the nucleus shielding (ppm) for the structures were calculated by using B3LYP/6-31G(d,p) level of theory. The NMR data are given in Table **3**.

Table 3: NMR analysis at B3LYP/6-31G(d,p) for azocubane isomers.

TAC		CAC	
Shielding (ppm)	Atoms	Shielding (ppm)	Atoms
-277.074	N1, N1'	-305.825	N1, N1'
27.075	H6, H6'	26.725	H3, H3'
27.341	H3, H3', H5, H5'	27.535	H5, H5', H6, H6'
27.745	H4, H4'	27.724	H7, H4'
27.856	H8, H8'	27.927	H4, H7', H8, H8', H9, H9'
28.024	H7, H7', H9, H9'	109.779	C2, C2'
105.180	C2, C2'	131.072	C5, C6'
135.792	C3, C3', C5, C5'	131.977	C6, C5'
138.067	C6, C6'	133.471	C3, C3'
140.801	C8, C8'	142.352	C8, C8'
145.886	C4, C4'	145.804	C4, C7'
146.040	C7, C7', C9, C9'	145.927	C7, C4'
-	-	146.593	C9, C9'

The IR spectrum is one basic property of a compound, and also an effective measure to identify structures [22]. Here, vibrational frequencies were calculated by using B3LYP/6-31G(d,p) level. Figure **3** provides structures' IR spectra.

Harmonic frequencies (cm^{-1}), IR intensities (KM/Mole)

CAC: 32.623 (1.003), 37.234 (0.089), 103.661 (0.080), 128.790 (0.0002), 153.392 (0.598), 236.765 (8.758), 241.021 (0.161), 480.525 (1.365), 491.155 (1.750), 529.905 (0.139), 615.251 (0.245), 628.457 (5.235), 636.590 (0.010), 648.466 (0.010), 691.263 (0.760), 691.565 (0.056), 696.436 (0.490), 699.262 (0.175), 743.460 (5.461), 771.468 (1.559), 787.277 (0.460), 833.126 (4.654), 835.142 (0.036), 844.611 (0.020), 845.993 (0.044), 849.294 (0.252), 849.758 (0.681), 856.194 (0.496), 856.643 (1.477), 861.688 (4.854), 863.770 (2.176), 870.008 (6.657), 871.115 (0.284), 901.523 (7.817), 909.203 (1.604), 909.551 (0.220), 912.033 (0.0001), 919.763 (2.632), 927.002 (10.360), 958.843 (10.729), 1009.225 (4.811), 1023.765 (1.893), 1025.664 (4.625), 1035.295 (0.042), 1054.583 (15.108), 1074.693 (3.708), 1075.730 (0.008), 1094.894 (0.141), 1096.972 (0.254), 1100.321 (0.087), 1101.491 (9.884), 1112.945 (0.024), 1117.444 (0.410), 1117.680 (1.610), 1124.389 (0.030), 1129.999 (0.004), 1135.237 (1.410), 1166.271 (0.547), 1167.399 (0.002), 1182.010 (0.013), 1184.428 (0.050), 1185.399 (0.011), 1187.477 (0.334), 1217.110 (3.247), 1218.168 (1.098), 1224.320 (1.880), 1224.957 (0.050), 1238.342 (0.310), 1243.299 (0.778), 1264.771 (2.236), 1267.507 (4.026), 1268.557 (1.533), 1269.978 (1.647), 1277.516 (1.604), 1285.605 (0.425), 1614.098 (31.983), 3119.276 (9.963), 3119.627 (6.845), 3125.836 (38.452), 3126.222 (14.462), 3130.848 (13.604), 3131.137 (37.653), 3133.724 (71.370), 3133.963 (62.067), 3138.121 (27.578), 3138.590 (73.700), 3146.782 (45.750), 3146.987 (72.845), 3159.244 (22.239), 3161.229 (10.236).

TAC: 26.499 (0.155), 61.128 (0.226), 68.831 (0.859), 407.825 (4.006), 728.175 (9.135), 546.898 (0.763), 646.249 (0.733), 650.498 (1.561), 695.546 (1.720), 696.048 (0.030), 795.217 (0.871), 836.744 (3.448), 843.343 (0.927), 847.219 (0.054), 851.297 (0.302), 863.604 (0.0001), 863.889 (9.735), 864.169 (7.572), 905.851 (3.075), 908.373 (2.969), 940.727 (5.779), 1025.484 (2.838), 1030.303 (0.548), 1052.955 (26.024), 1075.024 (0.323), 1090.901 (3.260), 1099.220 (0.236), 1114.039 (2.725), 1126.095 (0.020), 1164.169 (0.061), 1182.299 (0.028), 1186.550 (0.002), 1223.725 (0.010), 1226.263 (7.453), 1257.949 (0.348), 1268.389 (3.341), 1268.555 (3.862), 1327.427 (8.163), 3119.182 (0.532), 3119.183 (3.358), 3126.210 (51.034), 3126.230 (0.0006), 3129.084 (64.317), 3129.109 (0.024), 3131.291 (151.973), 3131.429 (0.036), 3136.651 (0.0006), 3137.113 (143.827), 3145.022 (108.395), 3163.089 (0.214), 3163.105 (27.954).

Ultraviolet–visible spectroscopy or ultraviolet-visible spectrophotometry (UV-Vis) refers to absorption spectroscopy or reflectance spectroscopy in the ultraviolet-visible spectral region. This means it uses light in the visible and adjacent (near-UV and near-infrared [NIR]) ranges [23]. The absorption or reflectance in the visible range directly affects the perceived color of the chemicals involved. In this region of the electromagnetic spectrum, molecules undergo electronic transitions [24]. Figure **4** shows the UV-Vis spectra of CAC and TAC. As seen from the data of Table **4**, the electron transition from HOMO-2 orbital to LUMO orbital of trans isomer of azocubane (TAC) is happened at 251.7 nm. In contrast, three electronic transitions are happened in CAC. The important one corresponds to the transition from

HOMO-1 orbital to LUMO orbital. It is observed this transition is done at 248.9 nm.

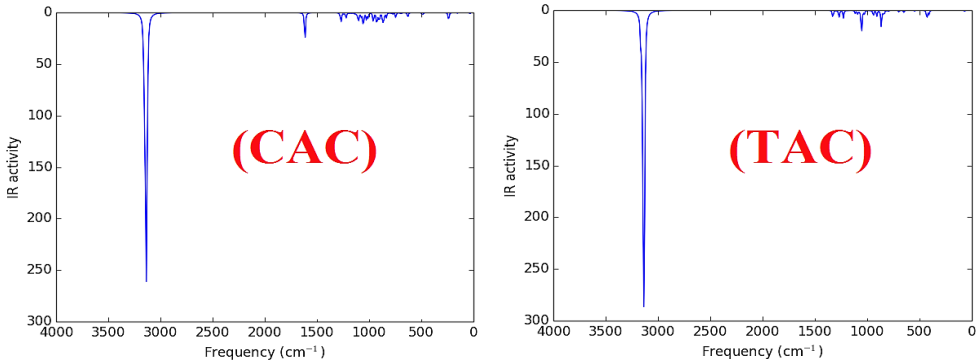

Figure 3: The IR spectra of CAC and TAC.

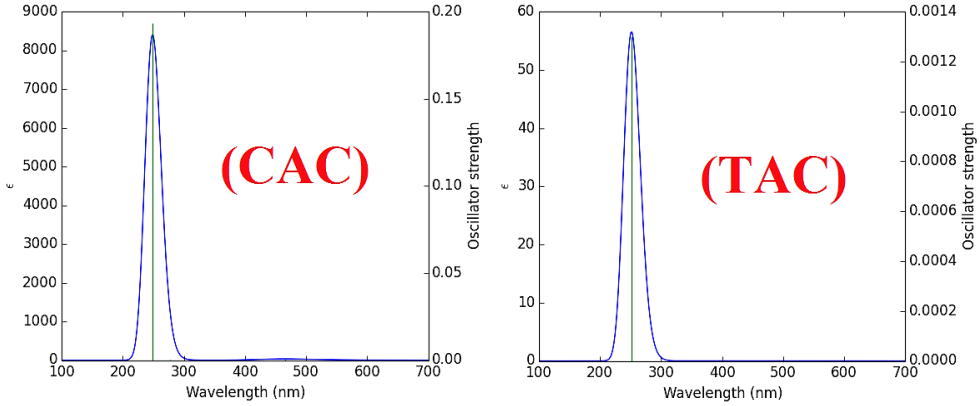

Figure 4: The UV-Vis spectra of CAC and TAC.

Table 4: The electronic transitions in CAC and TAC.

Compound	Transition	Energy (cm^{-1})	Wavelength (nm)	Strength
TAC	HOMO-2 → LUMO	39729.532	251.702	0.0013
	HOMO → LUMO	21493.211	465.263	0.0007
CAC	HOMO-2 → LUMO	36087.914	277.101	0.0003
	HOMO-1 → LUMO	40182.819	248.863	0.1931

Circular dichroism (CD) spectroscopy is a spectroscopic technique where the CD of molecules is measured over a range of wavelengths. Measurements carried out in the visible and ultra-violet region of the electro-magnetic spectrum monitor electronic transitions, and, if the molecule under study contains chiral chromophores then one circularly polarized light (CPL) state will be absorbed to a greater extent than the other and the CD signal over the corresponding wavelengths will be non-zero. A circular dichroism signal can be positive or negative, depending on whether left-handed circularly polarized light (L-CPL) is absorbed to a greater extent than right-handed circularly polarized light (R-CPL) (CD signal positive) or to a lesser extent (CD signal negative) [25]. It can be seen from the Figure **5**, CAC and TAC are left-handed and right-handed molecules, respectively.

Total energies (E), enthalpies (H) and Gibbs free energies (G) were calculated for the cis and trans isomers of azocubane via B3LYP/6-31G(d,p). As can be seen from the data of Table **5**, the trans isomer (TAC) is more stable. From our calculations, the difference between trans and cis configuration energies is 13.178 kcal/mol. And also, the equilibrium constant *k* of both the most stable trans and cis configurations is given in Table **5**. The equilibrium constant was obtained using formula [26]:

$$k = e^{\frac{-\Delta G}{RT}}$$

Where the ΔG is difference in the Gibbs energies of cis and trans configurations, T is temperature and R is gas constant. The equilibrium constant for the most stable configurations of azocubane is 1.76×10^{10}.

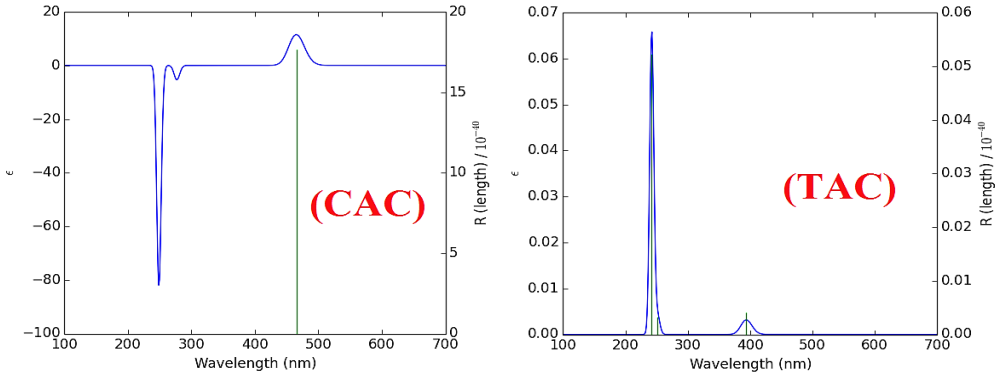

Figure 5: The CD spectra of CAC and TAC.

Table 5: Sum of electronic and thermal energy (E), sum of electronic and thermal enthalpy (H), sum of electronic and thermal free energy (G) at B3LYP/6-31G(d) for cis and trans isomers of azocubane.

Compound	E (a.u.)	ΔE (kcal/mol)	H (a.u.)	ΔH (kcal/mol)	G (a.u.)	ΔG (kcal/mol)	*K*
TAC	-726.6703	-13.178	-726.6684	-13.178	-726.7723	-13.742	1.76×10^{10}
CAC	-726.6493		-726.6474		-726.7504		

Dipole moment can be defined as the product of magnitude of charges and the distance of separation between the charges. The dipole moment of molecule was obtained by following formula [27]:

$$p = p_0 + \alpha E + \frac{1}{2}\beta EE + \cdots$$

Where p_0 is adipole moment without an electric field, α is a polarizability second-order tensor, β is the first in an infinite series of hyperpolarizabilities. The polarizability tensor was firstly diagonalized and mean and anisotropic polarizabilities have been obtained using following formulas [28]:

$$\alpha_{mean} = \frac{1}{3}(\alpha_{xx} + \alpha_{yy} + \alpha_{zz})$$

$$\alpha_{anis} = \sqrt{\frac{(\alpha_{xx} - \alpha_{yy})^2 + (\alpha_{yy} - \alpha_{zz})^2 + (\alpha_{xx} - \alpha_{zz})^2}{2}}$$

Where α_{xx}, α_{yy}, α_{zz} are diagonal elements of polarizability matrix. From the data of the Table **6**, the cis configuration of azocubane has big mean and anisotropic polarizabilities.

Table 6: Calculated dipole moments μ (Debye), mean and anisotropic polarizabilities α (a.u.) of the most stable trans and cis configurations obtained from B3LYP/6-31G(d) computations.

Compound	μ	Δμ	α_{mean}	Δα mean	α_{anis}	Δα anis
TAC	0.00	3.18	98.44	3.29	7.39	5.94
CAC	3.18		101.73		13.33	

Table **7** shows the HOMO and LUMO energies (***ε***) of the trans and cis configurations of the azocubane computed at B3LYP/6-31G(d,p) level of theory. It is observed that the gap energy of frontier orbitals in TAC is more than the gap enegy of HOMO and LUMO orbitals in CAC. It can be deduced the trans configuration of azocubane is more stable than the cis configuration of azocubane. The hardnesses (η), electronegativities (χ) and chemical potentials (μ) of the molecules were obtained using following formulas [29]:

$$\eta = \frac{(\varepsilon_{LUMO} - \varepsilon_{HOMO})}{2}$$

$$\chi = \frac{-(\varepsilon_{LUMO} + \varepsilon_{HOMO})}{2}$$

$$\mu = \frac{(\varepsilon_{LUMO} + \varepsilon_{HOMO})}{2}$$

It can be concluded from the data of the Table **7**, CAC is more reactive than TAC.

Density of states (DOS) of a system describes the number of states per interval of energy at each energy level that are available to be occupied. For atoms or molecules in gas phase, the density distributions are not discrete like a spectral density but continuous. A high DOS at a specific energy level means that there are many states available for occupation. A DOS of zero means that no states can be occupied at that energy level. In general a DOS is an average over the space and time domains occupied by the system [30].

Table 7: HOMO/LUMO energies, hardnesses (η), electronegativities (χ) and chemical potentials (μ) of the most stable trans and cis configurations obtained from B3LYP/6-31G(d,p) calculations.

Compounds	HOMO (eV)	LUMO (eV)	GAP (eV)	χ (eV)	μ (eV)	η (eV)
TAC	-5.71	-0.96	4.75	3.335	-3.335	2.375
CAC	-5.33	-1.23	4.10	3.280	-3.280	2.050

The DOS of investigated isomers (Figure **6**) were calculated and created by convoluting the molecular orbital information with Gaussian curves of unit height and full width at half maximum (FWHM) of 0.3 eV using GaussSum 3 [31]. As can be seen in Figure **6**, the CAC compound mainly uses the LUMO orbitals. In contrast, the TAC molecule mainly uses the HOMO orbitals. It is useful to remember at this step that LUMO represents the ability to obtain an electron, while HOMO represents the ability to donate an electron. Thus, the cis configuration of azocubane simply reacts with some other system by obtaining an electron.

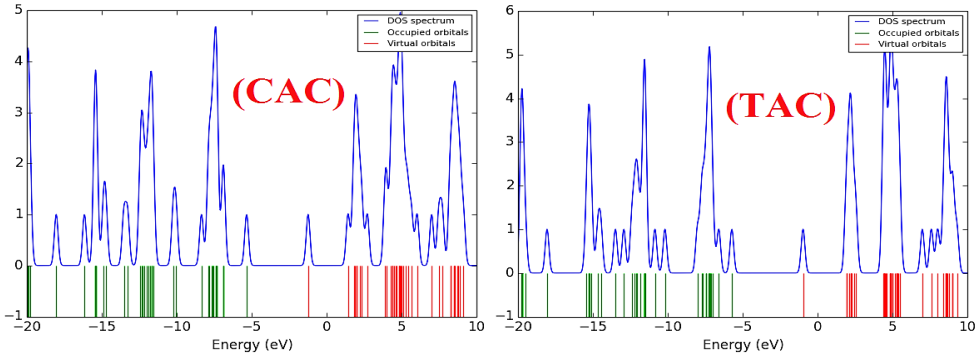

Figure 6: DOS plots of CAC and TAC.

Detonation velocity (D) and detonation pressure (P) are the two most important parameters determining the brisance of explosive materials. Based on the estimated solid phase heat of formation and crystal density, the values of D and P calculated using Kamlet-Jacobs equations (following equations) [32] are listed in Table **8**.

$$D=1.01(NM^{1/2}Q^{1/2})^{1/2}(1+1.3\rho)$$
$$P=1.558\rho^{2}NM^{1/2}Q^{1/2}$$

Stoichiometric ratio*

parameters	c≥2a+b/2	2a+b/2>c≥b/2	b/2>c
N	(b+2c+2d)/4MW	(b+2c+2d)/4MW	(b+d)/2MW
M	4MW/(b+2c+2d)	(56d+88c-8b)/(b+2c+2d)	(2b+28d+32c)/(b+d)
Q	(28.9b+94.05a+0.239ΔHf̊)/MW	[28.9b+94.05(c/2-b/4)+0.239ΔHf̊]/MW	(57.8c+0.239ΔHf̊)/MW

*a, b, c and d correspond to the number of carbon, hydrogen, oxygen and nitrogen,respectively.

Where D: detonation velocity in km/s, P: detonation pressure in GPa, ρ: density of a compound in g/cm^3, N: moles of gaseous detonation products per gram of explosive (in mol/g), M: average molecular weight of gaseous products (in g/mol), Q: chemical energy of detonation in kJ/g.

The data show that the heat of detonation, crystal density, and detonation velocity and detonation pressure of CAC are lower as compared to TAC.

Table 8: HOFs, predicted densities and detonation properties of the molecules.

Structures	M_w (amu.)	OB_{100}	HOF (kJ/mol)	Q (kJ/g)	V* (cm^3/mol)	ρ (g/cm^3)	D (km/s)	P (GPa)
TAC	234.1157	-266.53	1792.409	1829.804	161.165	1.453	5.340	11.016
CAC			1735.811	1772.025	163.769	1.430	5.242	10.501

*Average valu from 100 single-point volume calculations at the B3LYP/6-311G(d,p) level.
Q: Heat of explosion, V: Volume of explosion, D: Velocity of detonation, P: Pressure of explosion.

Conclusion

In the present study, the two most stable configurations of azocubane (CAC and TAC) were designed and their stability, reactivity, detonation and electronic structure characteristics have been determined and the following conclusions drawn:

(1) The C-N-N-C torsion angle for cis configuration is longer than the one of trans configuration.

(2) The negative charge is located on the nitrogen elements of molecules as expected due to the electron withdrawing character of theirs and positive charge is located on the cubane sections of the structures.

(3) CAC and TAC are left-handed and right-handed molecules, respectively.

(4) TAC is more stable configuration of azocubane.

(5) The reactivity of CAC is more than the reactivity of TAC.

(6) CAC and TAC mainly use the LUMO and HOMO orbitals, respectively.

(7) Predicted values of detonation parameters of TAC are more to those of CAC.

Experimental

Computational method:

Computations were carried out with the Gaussian 03 package [33] using the B3LYP method with 6-31G(d,p) basis set. All calculations and geometry optimization for each molecule were obtained by mentioned theory (B3LYP). The designation of B3LYP consists of the Vosko, Wilk, Nusair (VWN3) local correlation functional [34] and the Lee, Yang, Parr (LYP) correlation correction functional [35, 36].

Acknowledgement

This work was supported by the Azarbaijan Shahid Madani University, Tabriz, Iran.

References

[1] Nabati, M.; Mahkam, M. *Iran. J. Org. Chem.* **2014,** *6*, 1331.
[2] Jursic, B. S. *J. Mol. Struct.* **2000,** *499*, 137.
[3] Mahkam, M.; Nabati, M.; Latifpour, A.; Aboudi, J. *Des. Monomers Polym.* **2014,** *17*, 453.
[4] Nabati, M.; Mahkam, M. *Silicon* **2016,** *8*, in press.
[5] Dismukes, G. C.; Brimblecombe, R.; Felton, G. A. N.; Pryadun, R. S.; Sheats, J. E.; Spiccia, L.; Swiegers, G. F. *Acc. Chem. Res.* **2009,** *42*, 1935.
[6] Hidai, M.; Kuwata, S. *Acc. Chem. Res.* **2000,** *33*, 46.
[7] Zhang, W.; Xiong, R.; Huang, S. D. *J. Am. Chem. Soc.* **2008,** *130*, 10468.
[8] McCool, N. S.; Robinson, D. M.; Sheats, J. E.; Dismukes, G. C. *J. Am. Chem. Soc.* **2011,** *133*, 11446.
[9] Mahkam, M.; Namazifar, Z.; Nabati, M.; Aboudi, J. *Iran. J. Org. Chem.* **2014,** *6*, 1217.
[10] Nabati, M.; Mahkam, M. *Iran. Chem. Commun.* **2014,** *2*, 164.
[11] Konstantinou, I. K.; Albanis, T. A. *Appl. Catal. B* **2004,** *49*, 1.
[12] Natansohn, A. *Chem. Rev.* **2002,** *102*, 4139.
[13] Lucas, M. S.; Peres, J. A. *Dyes Pigm.* **2006,** *71*, 236.
[14] Viswanathan, N. K.; Kim, D. Y.; Bian, S.; Williams, J.; Liu, W.; Li, L.; Samuelson, L.; Kumar, J.; Tripathy, S. K. *J. Mater. Chem.* **1999,** *9*, 1941.
[15] Egami, C.; Suzuki, Y.; Sugihara, O.; Okamoto, N.; Fujimura, H.; Nakagawa, K.; Fujiwara, H. *Appl. Phys. B* **1997,** *64*, 471.
[16] Statman, D.; Janossy, I. *J. Chem. Phys.* **2003,** *118*, 3222.
[17] Folcia, C. L.; Alonso, I.; Ortega, J.; Etxebarria, J.; Pintre, I.; Ros, M. B. *Chem. Mater.* **2006,** *18*, 4617.
[18] Nabati, M.; Mahkam, M. *Iran. J. Org. Chem.* **2014,** *6*, 1397.
[19] Nabati, M.; Mahkam, M. *Iran. J. Phys. Theor. Chem. IAU Iran* **2015,** *12*, 33.
[20] Türker, L. *J. Mol. Struct. (Theochem)* **2004,** *681*, 15.
[21] Turker, L.; Atalar, T.; Gumus, S.; Camur, Y. *J. Hazard. Mater.* **2009,** *167*, 440.
[22] Upadhyay, M. K.; Sengupta, S. K.; Singh, H. J. *J. Mol. Model.* **2015,** *21*, 18.
[23] Kayi, H. *J. Mol. Model.* **2014,** *20*, 2269.
[24] Piyanzina, I.; Minisini, B.; Tayurskii, D.; Bardeau, J. F. *J. Mol. Model.* **2015,** *21*, 34.
[25] Vessally, E. *Bull. Chem. Soc. Ethiop.* **2009,** *23*, 223.
[26] Hou, L. J.; Wu, B. W.; Han, Y. X.; Kong, C.; Chen, D. P.; Gao, L. G. *Comput. Theor. Chem.* **2015,** *1051*, 57.
[27] Gutierrez-Arzaluz, L.; Roch-Rinza, T.; Cortes-Guzman, F. *Comput. Theor. Chem.* **2015,** *1053*, 214.
[28] Huang, J.; He, C.; Liu, C.; Tong, H.; Wu, L.; Wu, S. *Comput. Theor. Chem.* **2015,** *1054*, 80.
[29] Junqueira, G. M. A.; Sato, F. *J. Mol. Model.* **2014,** *20*, 2275.
[30] Sun, S.; Zhang, K.; Lu, Y.; Wang, A.; Zhang, H. *J. Mol. Model.* **2014,** *20*, 2288.
[31] O'Boyle, N. M.; Tenderholt, A. L.; Langner, K. M. *J. Comp. Chem.* **2008,** *29*, 839.
[32] Kamlet, M. J.; Jacobs, S. J. *J. Chem. Phys.* **1968,** *48*, 23.
[33] Frisch, M. J.; Trucks, G. W.; Schlegel, H. B.; Scuseria, G. E.; Robb, M. A.; Cheeseman, J. R.; Montgomery Jr., J. A.; Vreven, T.; Kudin, K. N.; Burant, J. C.; Millam, J. M.; Iyengar, S. S.; Tomasi, J.; Barone, V.; Mennucci, B.; Cossi, M.; Scalmani, G.; Rega, N.; Petersson, G. A.; Nakatsuji, H.; Hada, M.; Ehara, M.; Toyota, K.; Fukuda, R.; Hasegawa, J.; Ishida, M.; Nakajima, T.; Honda, Y.; Kitao, O.; Nakai, H.; Klene, M.; Li, X.; Knox, J. E.; Hratchian, H. P.; Cross, J. B.; Adamo, C.; Jaramillo, J.; Gomperts, R.; Stratmann, R. E.; Yazyev,

O.; Austin, A. J.; Cammi, R.; Pomelli, C.; Ochterski, J. W.; Ayala, P. Y.; Morokuma, K.; Voth, G. A.; Salvador, P.; Dannenberg, J. J.; Zakrzewski, V. G.; Dapprich, S.; Daniels, A. D.; Strain, M. C.; Farkas, O.; Malick, D. K.; Rabuck, A. D.; Raghavachari, K.; Foresman, J. B.; Ortiz, J. V.; Cui, Q.; Baboul, A. G.; Clifford, S.; Cioslowski, J.; Stefanov, B. B.; Liu, G.; Liashenko, A; Piskorz, P.; Komaromi, I.; Martin, R. L.; Fox, D. J.; Keith, T.; Al-Laham, M. A.; Peng, C. Y.; Nanayakkara, A.; Challacombe, M.; Gill, P. M. W.; Johnson, B.; Chen, W.; Wong, M. W.; Gonzalez, C.; Pople, J. A. *Gaussian 03. Revision B.01*. Gaussian Inc. Wallingford. CT. **2004**.

[34] Vosko, S. H.; Wilk, L.; Nusair, M. *Can. J. Phys.* **1980,** *58*, 1200.

[35] Lee, C.; Yang, W.; Parr, R. G. *Phys. Rev. B* **1988,** *37*, 785.

[36] Miehlich, B.; Savin, A.; Stoll, H.; Preuss, H. *Chem. Phys. Lett.* **1989,** *157*, 200.